kcal/mol; ΔS_a = –16 cal/(K mol)) also shows that the N-methyl compound has smaller values for these parameters. According to arguments presented in the preceeding paragraph, points 3 and 4 suggest stronger anion–solvent interaction for the N-methyl compounds.

There is strong evidence that the observed variations in ΔH_a and ΔS_a are due to water solvent interactions with the –[C(=O)N(O$^-$)–] moiety rather than with the substituents on the C and/or N atoms. This is nicely illustrated by the comparison of the two pairs of geometric isomers shown in Table II. Significant differences in ΔH_a and ΔS_a values are found for both pairs of isomers, despite the identical substituents for each isomeric pair. Making the reasonable assumption that solvation of these substituents should be the same regardless of attachment to C or N, these isomer comparisons strongly support our arguments concerning solvent interactions specifically with the hydroxamate moiety, which is influenced by the substituents on the C and/or N atom.[28]

(27) Reference 7 contains pK_a data obtained at various temperatures in an ethanol/water solvent mixture for a series of hydroxamic acids; the authors did not use these data to calculate ΔS or ΔH values. The 25 °C pK_a values are in excellent agreement with 25 °C pK_a values determined in 100% water in ref 8 for the same hydroxamic acids. We therefore have used the temperature-dependent data of ref 7 to calculate ΔH_a and ΔS_a for 4-NO$_2$C$_6$H$_4$C(O)N(OH)H. These values were used in our analysis without further correction for differing conditions, and, therefore, some caution should be exercised in the comparative analysis. However, the ΔH_a and ΔS_a values calculated for 4-NO$_2$C$_6$H$_4$C(O)N(OH)H fall on the linear ΔH_a–ΔS_a correlation shown in Figure 1 for the 17 hydroxamic acids investigated in our laboratory and which were investigated by a common technique and set of experimental conditions.

(28) Although the steric environments about the carbon and nitrogen differ in these isomers, we propose that any contribution to the differences in ΔH_a and ΔS_a of these isomer pairs by steric effects in the undissociated acids is negligible compared to the electronic influence of the substituents on the solvation of the anion. This is supported by the large changes in ΔH_a and ΔS_a ($\Delta\Delta H_a \approx 6$ kcal/mol and $\Delta\Delta S_a \approx 17$ cal/(K mol)) among the substituted N-phenylacetohydroxamic acids (compounds 9–17 in Figure 1) which would show no steric differences at the C and N atoms. Furthermore, if the bulk of the substituent on the N would alter hydrogen bonding about the N enough to effect the solvation of the anion, one would expect a reasonable progression to exist between ΔH_a and ΔS_a and the bulk of the substituent. This is not found to be the case for CH$_3$C(O)N(OH)H, CH$_3$C(O)N(OH)CH$_3$, and CH$_3$C(O)N(OH)C$_6$H$_5$,[2,3] where R$_2$ is varied from H to CH$_3$ to C$_6$H$_5$. This is consistent, then, with our argument that the variations in ΔH_a and ΔS_a are produced by the electronic effects of the substituents and not steric effects.

(29) King, E. J. In "The International Encyclopedia of Physical Chemistry and Chemical Physics"; Topic 15, Guggenheim, E. A., Mayer, J. E.; Tompkins, F. C., Eds.; The MacMillan Co.: New York, 1965; Vol. 4, Topic 15, p 194.

Structural Effects in Phosphates. 1. Comparison of 4-Nitrophenyl 1-Naphthyl and 4-Nitrophenyl Quinolin-8-yl Phosphates

D. R. Bond, T. A. Modro,* and L. R. Nassimbeni*

School of Chemical Sciences, University of Cape Town, Rondebosch, South Africa

Crystal and molecular structures of quinolin-8-yl bis(p-nitrophenyl) (4), quinolin-8-yl p-nitrophenyl (4a), and 1-naphthyl bis(p-nitrophenyl) phosphates (5) have been determined and compared. In 4 the donor–acceptor nitrogen–phosphorus interactions change the geometry of the molecule from tetrahedral to quasi-tbp, so the structure can be considered as an "early stage" of the intramolecular displacement of the PNPO group. In 4a this interaction is replaced by intramolecular N··H··O hydrogen bonding. The intramolecular nonbonded potential energies of 4 and 5 were calculated, and the minimum-energy conformations obtained were compared with those determined by X-ray diffraction. The results of calculations confirm the observed differences in the intramolecular interactions operating in 4 and 5. The mass spectra of 4 and 5 reveal a dramatic difference between these two phosphates with respect to the fragmentation involving the expulsion of the p-nitrophenoxy radical and the formation of the corresponding phosphorylium ion by the nitrogen atom. Rate measurements for the base-catalyzed hydrolysis of the P–OPNP linkage show that 4 is not significantly more reactive than 5 and provide no evidence for the intramolecular nucleophilic catalysis in the hydrolysis of 4.

Intramolecular nucleophilic catalysis in the displacement at the phosphoryl substrates attracts considerable attention.[1] Loran and Williams demonstrated[2] that the hydrolysis of 4-nitrophenyl quinolin-8-yl phosphate (1) involves expulsion of 4-nitrophenoxide via intramolecular nucleophilic attack to give a cyclic intermediate (2). This results in ca. a 350-fold rate increase for the hydrolysis of 1 relative to the reactivity of 4-nitrophenyl phenyl phosphate.
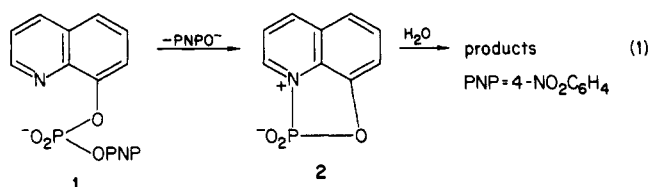

As a continuation of our investigation of structural correlations in organophosphorus chemistry,[3] we were interested to see whether the nitrogen–phosphorus interac-

(1) Lazarus, R. A.; Benkovic, P. A.; Benkovic, S. J. *J. Chem. Soc. Perkin Trans. 2*, **1980**, 373 and references cited therein.
(2) Loran, J. S.; Williams, A. *J. Chem. Soc. Perkin Trans. 2*, **1977**, 64.

(3) Archer, S. J.; Modro, T. A.; Nassimbeni, L. R. *Phosphorus Sulfur* **1981**, *11*, 101.

tions responsible for the intramolecular catalysis in the hydrolysis of phosphates derived from 8-hydroxyquinoline manifest themselves in the molecular parameters of a substrate. The intramolecular displacement of the leaving group L by nitrogen in the quinolin-8-yl phosphate (eq 2)

$$(2)$$
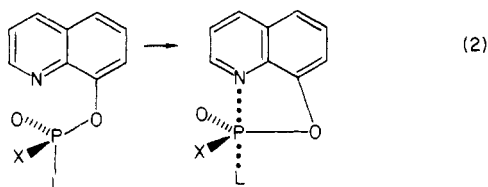
involves a change in the phosphorus geometry from tetrahedral to trigonal bipyramidal, accompanied by the necessary modifications in bond lengths and angles. If the molecular structure of a suitably selected model compound would reveal the presence of such interactions, the structure could then be considered as an "early stage"[4] of the intramolecular displacement at the P^{IV} atom. Schmutzler and co-workers have demonstrated[5] that fluorophosphoranes (3) exist as hexacoordinated phosphorus species with almost perfect octahedral geometry. The P–N bond distance in 3 is in the range of 1.9–2.0 Å, not much longer than the value of 1.77 Å reported[6] for the "pure" P–N σ bond. The close approach of nitrogen to phosphorus in 3, despite the considerable distortion of the quinoline skeleton required, certainly results from the presence of three (or four) fluorine atoms of the P^V center.

3, X = F or Ph
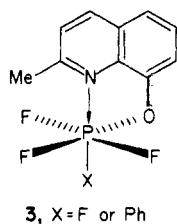
In this work we wish to report on the structural effects operating in bis(4-nitrophenyl) quinolin-8-yl phosphate (4) and to compare this ester with its 1-naphthyl analogue (5) in which no specific intramolecular interactions can be expected. We have related structural parameters of
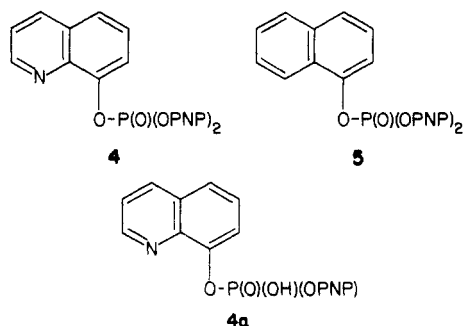
molecules 4 and 5 to independently obtained sets of reactivity data. Firstly, we have calculated the intramolecular nonbonded potential energy of 4 and 5 and compared the conformations corresponding to the minima in total intramolecular energy (TIE) with those determined by X-ray diffraction. Secondly, we compared the fragmentation patterns of phosphates 4 and 5 resulting from
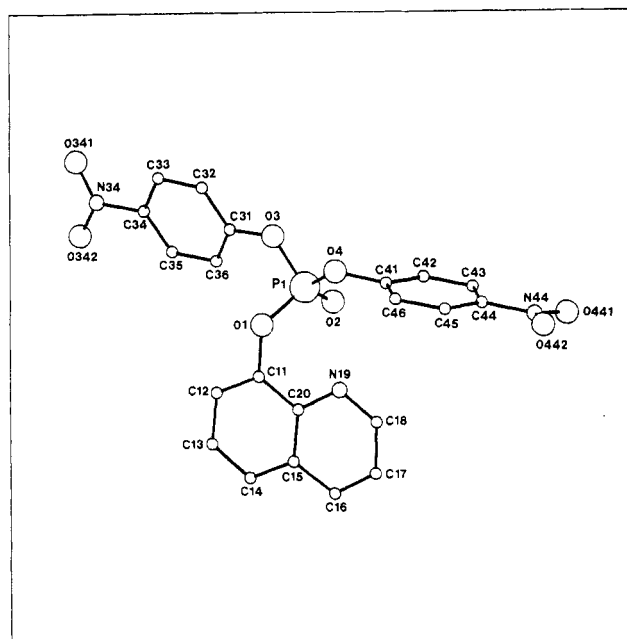
(4) Bürgi, H. B.; Dunitz, J. D. *Acc. Chem. Res.* **1983**, *16*, 153.
(5) (a) John, K. P.; Schmutzler, R.; Sheldrick, W. S. *J. Chem. Soc., Dalton Trans.* **1974**, 1841. (b) Ibid. **1974**, 2466.
(6) Cruickshank, D. W. J. *Acta Crystallogr.* **1964**, *17*, 671.

Figure 1. Perspective view of quinolin-8-yl bis(*p*-nitrophenyl) phosphate (4).

Table I. Selected Interatomic Distances (Å) and Bond Angles (deg) in 4, 5, and 4a (Standard Deviations Shown in Parentheses)

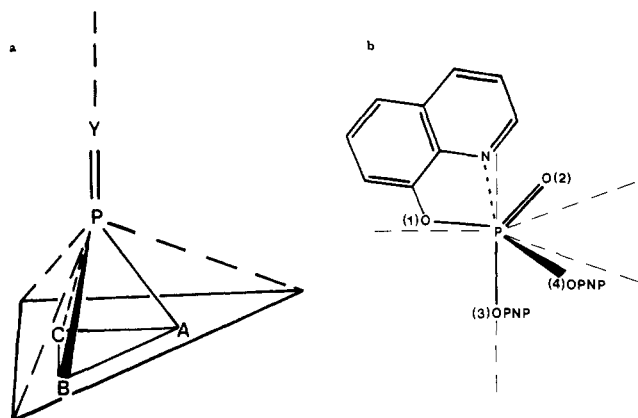| distances	4	5	4a
P–O(1)	1.571 (3)	1.560 (2)	1.622 (5)
P–O(2)	1.447 (3)	1.446 (2)	1.473 (4)
P–O(3)	1.586 (3)	1.568 (2)	1.628 (4)
P–O(4)	1.560 (3)	1.569 (1)	1.457 (4)
O(1)–C(11)	1.414 (6)	1.420 (3)	1.398 (6)
O(3)–C(31)	1.387 (5)	1.411 (3)	1.381 (7)
O(4)–C(41)	1.407 (5)	1.402 (4)	
angles	4	5	4a
O(2)–P–O(1)	116.2 (2)	117.5 (1)	104.1 (3)
O(2)–P–O(3)	116.5 (2)	116.8 (1)	109.8 (2)
O(2)–P–O(4)	118.3 (2)	115.3 (1)	124.4 (3)
O(1)–P–O(3)	99.5 (2)	102.4 (1)	101.0 (2)
O(1)–P–O(4)	107.6 (2)	101.4 (1)	110.5 (3)
O(3)–P–O(4)	95.3 (2)	100.9 (1)	104.8 (3)
intermolecular nonbonded distances and angles	4	5	4a
N(19)···P	3.019		
N(19)····P–O(3)	158.8		
C(19)····P		3.790	
C(19)····P–O(3)		127.3	
N(19)····O(2)[a]			2.610

[a] $1 - x, 1 - y, 1 - z$.

electron impact, and their reactivity toward the base-catalysed hydrolysis of the P–OPNP ester linkage. We thus hoped to provide some information on the effect of the neighboring nitrogen atom on the structure and dynamics of phosphate esters containing a good leaving group.

Finally, we have compared the structure of 4 with that determined for its hydrolysis product—(4-nitrophenyl) quinolin-8-yl phosphate (4a). Since hydrolysis of 4 results in the introduction of an acidic hydrogen into the molecule, the nitrogen atom would be expected to be involved in hydrogen bonding rather than in the interactions with the phosphoryl center. We were interested in effects of these changes of functional groups on the molecular structure of the phosphate.

Figure 2. (a) Distortion of the tetrahedral geometry in ABCP=Y molecule. Dashed lines represent the ideal tetrahedral geometry. (b) Distortion of the tbp geometry in 4. Dashed lines represent ideal tbp geometry.

Results and Discussion

Molecular Structures. Selected bond lengths and angles obtained for substrates **4, 5,** and **4a** are listed in Table I; Figure 1 depicts a perspective view of the molecule **4** with atomic nomenclature.

The phosphorus atom in both tertiary substrates has a geometry reasonably close to the regular tetrahedral; the average values for all O–P–O angles for **4** and **5** are 108.9° and 109.1°, respectively. The individual angles of phosphorus show, however, considerable deviations from the average value (±9.7° for **4** and ±8.2° for **5**), and for each phosphate they can be grouped into three "wide" (117.0 ± 1.1° for **4** and 116.5 ± 1.1° for **5**) O=P—OAr and three "narrow" (100.8 ± 6.2° for **4** and 101.6 ± 0.8° for **5**) Ar-O—P—OAr angles. These deviations follow the same pattern observed for other P^{IV} derivatives of the ABCP=Y type, which results in the distortion of the tetrahedral geometry at phosphorus as illustrated in Figure 2 part a. The deviations of bond angles from the ideal value of 109.5° result from the greater repulsions involving multiple bonding orbitals[7] and can be correlated with the corresponding bond distances.[8]

In this respect, substrates **4** and **5** resemble each other and the "orbitals repulsion" effect seems to be a dominating one in governing the molecular geometry. However, it is easy to see that in the quinoline derivative **4** additional effects are present, superimposed on the effect discussed above, common to all phosphates. The values of the "narrow" (ArO–P–OAr) angles for **4** show a scatter almost of an order of magnitude greater than the analogous values for the reference compound **5**. This is due to the nitrogen atom, which interacts strongly, as expected, with the phosphoryl center. The nitrogen–phosphorus nonbonded distance in **4** is 3.02 Å, while the corresponding sum of the van der Waals radii is 3.44 Å. This short contact, although still longer than that of ca. 2 Å observed by Schmutzler et al.[5] for fluorophosphoranes, clearly indicates intramolecular, nucleophilic approach of nitrogen to phosphorus and is expected to change the geometry of the molecule toward that of a trigonal bipyramid. Structure **4** indeed shows some features of the P^V tbp system. One of the 4-nitrophenoxy groups tends to apical geometry: the P–O(3) bond is slightly longer than the P–O(4) bond[9] and N···P–O(3) angle of 159° is approaching the idealised value of 180°. Also the "quasi-apical" O(3)PNP group makes
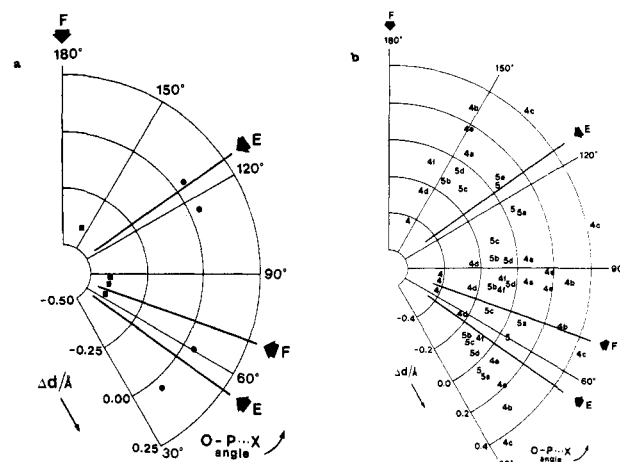
Figure 3. (a) P···N distance vs. O–P···N angles for **4** (squares) and P···C(19) distance vs. O–P···C(19) angles for **5** (circles). (b) P···X distance vs. O–P···X angles for **4, 4a–f** (X = N) and for **5, 5a–d** (X = CH).

angles of 99.5° and 95.3° with the "quasi-equatorial" O(1) and O(4) atoms, tending toward the ideal 90°. It is only the phosphoryl group which deviates strongly from its expected "quasi-equatorial" position. As a result of these two overlapping effects, the geometry of **4** can be schematically represented by Figure 2 part b.

The difference in the intramolecular interactions operating in the two phosphates can be demonstrated additionally by comparing the orientation of the nitrogen atom in **4** with respect to the P^{IV} center, with the analogous orientation of the C19 atom in **5**. If the quinoline nitrogen is considered as an internal nucleophile, it should, in agreement with the generally accepted[10] stereochemistry of nucleophilic substitution, approach the phosphoryl center according to the so called "face" attack. For the ideal "face" approach by a nucleophile (NU) to the tetrahedral phosphate center, the O–P····Nu angles are 180° (one) and 70.5° (three); the alternative "edge" orientation requires two O–P····Nu angles of 54.7° and two of 125.3°. Figure 3 part a gives the plot of the phosphorus–nitrogen (or phosphorus–C19) distance vs. four O–P···N (or O–P···C19) angles for phosphates **4** and **5**.

The P–Y (Y = N or C19) distance Δd is given relative to the sum of Van der Waals radii, so $\Delta d = 0$ represents the distance corresponding to the sum of the Van der Waals radii of atoms P and Y. Figure 3 part a demonstrates that in **4** close ($\Delta d < 0$) and "face" approach is chosen by the nitrogen atom, as expected for the "early stage" of nucleophilic substitution. In **5** the α-carbon of the naphthalene ring (C19) locates itself at a longer range ($\Delta d > 0$) from the phosphoryl center, with the "edge" orientation, which is not typical for the nucleophile–electrophile interaction.

As expected, hydrolysis of one of the PNPO–P functions in **4** (diester structure **4a**) has a profound effect on the molecular structure of the whole system. The phosphorus atom in **4a** remains tetrahedral average O–P–O angle = 109.1 ± 8.3°), but it is now the negative charge introduced to the phosphate group which determines the deviations of individual bond angles from the regular tetrahedral values. The electrostatic repulsion between two negatively charged oxygen atoms results in the increase of the O-(2)–P–O(4) angle to the value of 124.4°, simultaneously compressing the angle (3)O–P–O(1) to 101°. The most

(7) Gillespie, R. J. *J. Chem. Ed.* **1963,** *40,* 295.
(8) Bond, D. R.; Nassimbeni, L. R.; Modro, T. A., unpublished results.
(9) The two P–OPNP bond lengths in **5** are identical.

(10) Emsley, J.; Hall, D. "The Chemistry of Phosphorus"; Harper and Row: New York, 1976; Chapter 8.2.

Table II. Intramolecular Parameters and Calculated Nonbonded Energies for 4, 5, and Their Conformers Corresponding to the Potential Energy Minima

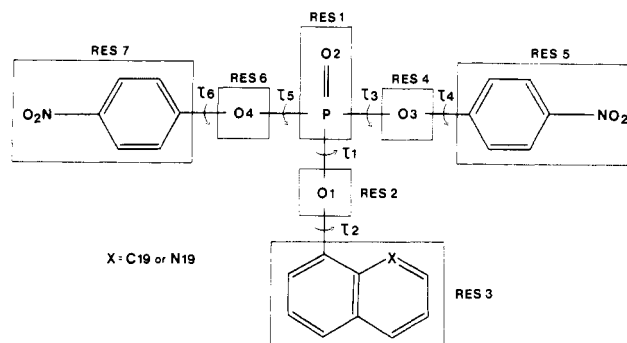|	4[a]	4a	4b	4c	4d	4e	4f	5[a]	5a	5b	5c	5d
P···Y (Å)[b]	3.019	3.486	3.723	3.873	3.197	3.612	3.362	3.790	3.811	3.608	3.629	3.697
Δd (Å)[c]	−0.421	+0.046	+0.283	+0.433	−0.243	+0.172	−0.078	+0.040	+0.061	−0.142	−0.121	−0.053
O1–P···Y (deg)	63.8	48.7	40.2	34.1	58.2	44.3	52.9	41.2	40.7	48.7	47.6	44.8
O2–P···Y (deg)	83.7	93.1	152.8	138.5	77.2	88.4	79.3	127.3	112.5	79.5	104.0	92.5
O3–P···Y (deg)	158.8	145.4	85.8	66.3	157.6	82.7	84.2	115.0	128.7	95.2	138.0	144.8
O4–P···Y (deg)	78.8	84.7	71.5	101.8	92.6	150.2	159.8	60.0	67.4	148.4	66.5	80.6
TIE (kcal mol⁻¹)	15.3	13.1	11.7	12.4	11.5	13.1	13.6	14.4	13.0	12.6	12.8	12.8

[a] Crystal structure. [b] Y = N or C19. [c] Sum of the van der Waals radii calculated by using values (Å):[17] N = 1.54; P = 1.90; C = 1.85.

important difference between the molecular structure of **4a** and its neutral precursor **4** is, however, the change in the nature of the intramolecular interactions involving the nitrogen atom. Diester **4a** exists as a zwitterion with the N^+–H function strongly hydrogen bonded to one of the negatively charged oxygen atoms in a neighboring molecule. This effect removes the nitrogen from the vicinity of the phosphorus atom and locates it close to the O(2)[i] atom, with a N(19)···O(2)[i] distance of 2.61 Å (as compared with the sum of the van der Waals radii of 2.95 Å). It is interesting to note that although formally both of the oxygen atoms of the PO_2^- group (O(2) and O(4)) are equivalent, the intermolecular hydrogen bonding to the N^+–H group makes these two oxygens clearly nonequivalent. The bond between phosphorus and the hydrogen-bonded O(2) has less multiple bond character and thus is longer (1.473 Å) than the P–O bond with the "free" negative oxygen (1.457 Å). The hydrogen bonding between the PO_2^- acceptor and the N^+–H donor groups is therefore unsymmetrical and involves essentially only one oxygen atom. This result, observed also for some other hydrogen-bonded phosphates,[11] gives evidence for the preferential formation of "linear" hydrogen bond, as opposed to the "bifurcated" hydrogen bond, predicted by recent theoretical calculations[12] to be more stable.

Conformational Study. We have carried out a conformational study of compounds **4** and **5** by calculating the van der Waals energy using empirical atom pair potentials. This method of evaluating molecular energies is well established and has recently been reviewed by Kitaigorodsky[13] and Mirsky.[14] The coefficients of the atom–atom potentials are of the form,

$$U(r) = a \exp(-br)/r^d - c/r^6 \quad (3)$$

where r is the distance between any pair of atoms and the coefficients a, b, c, and d are those given by Giglio,[15] such that $U(r)$ is evaluated in calories when r is in Å. These potential energy curves were derived primarily to give good agreement for calculation of molecular position in a crystal structure and the energy values mean little in an absolute sense. No account was taken of possible torsional potentials for sigma bonds, partial atomic charges, or dipole interactions. The program EENY[16] calculates molecular coordinates as defined by appropriate torsion angles and sums the energy for all nonbonded pairs of atoms whose

(11) Bond, D. R.; Modro, T. A.; Nassimbeni, L. R.; Niven, M., in preparation.

(12) Aragona, G.; Ghio, C.; Kollman, P. *J. Am. Chem. Soc.* **1983**, *105*, 5226.

(13) Kitaigorodsky, A. I. *Chem. Soc. Rev.* **1978**, *7*, 133.

(14) Mirsky, K. In "Computing in Crystallography"; Schenk, K., Olthof-Hazekamp, R., van Koningsveld, H., Bassi, G. C., Eds.; Delft University Press: Delft, 1978.

(15) Giglio, E. *Nature (London)* **1969**, *222*, 339.

(16) Motherwell, W. D. S. EENY Potential Energy Program, Cambridge University.

(17) "Lange's Handbook of Chemistry", 11th ed.; Dean, J. A., Ed.; McGraw-Hill: New York, 1973.

Figure 4. Structures **4** and **5** divided into seven residues.

separation is dependent upon the torsion angles.

Structures **4** and **5** were analyzed by initially dividing the molecules into seven residues linked by six torsion angles shown in Figure 4. We did not carry out a full six-dimensional mapping by varying all six torsion angles simultaneously, but approximated our analysis by initially omitting residues 5 and 7, and calculating an energy map by varying torsion angles τ_1 and τ_2. The resulting map yielded four distinct energy minima.

With τ_1 and τ_2 fixed at each of these minima, further maps were then calculated by varying τ_4 and τ_6. In this way we located all the important energy valleys and the torsion angles and final energies were refined by a method of steepest descent incorporated in the program. The results of our analysis are summarised in Table II and Figure 3 part b.

Compound **4** yielded six conformations different from the crystal structure, all having similar total intramolecular nonbonded energies (TIE). If one regards the *p*-nitrophenoxide (PNPO⁻) leaving groups as equivalent, then the geometries of the conformations all approximate a face approach and are such that the quinolyl nitrogen, N(19), lies roughly opposite O(3) in conformers **4a** and **4d** and opposite O(4) in conformers **4e** and **4f**. Conformers **4b** and **4c** are chemically less interesting, in that N(19) lies opposite the phosphoryl oxygen, O(2). Interestingly, the conformer given by the crystal structure is the one which best models the incipient S_N2 mechanism via a tbp intermediate, as being the one with the closest P···N(19) distance. Compound **5** yielded four conformations besides the crystal, again all of similar energies. While the conformation in the solid state and that closely related to it, **5** and **5a**, respectively, show an edge approach of C(19) to the phosphorus, the other conformers, **5b**, **5c**, and **5d**, have geometries which lie between an edge and a face approach. We note that none of the conformers of compound **5** approach the tbp geometry and that the C(19)···P distances are never significantly lower than the sum of the van der Waals radii. This is in accordance with the expected nonparticipation of C(19) in intramolecular catalysis.

Fragmentation Behavior. Principal modes of fragmentation of aromatic phosphate triesters $(ArO)_3PO$ result in the formation of the following primary products:[18] (i)

ArOH+·(P–O cleavage with H migration); (ii) $(ArO)_2PO^+$ (P–O cleavage, loss of ArO·); (iii) Ar+ (C–O cleavage, loss of $(ArO)_2PO_2^+$); (iv) $(ArO)_2PO_2^+$ (C–O cleavage, loss of Ar·). The most relevant for our discussion is fragmentation ii yielding the phosphorylium ion $(ArO)_2PO^+$ **6**. We have found the dramatic difference in the behavior of phosphates **4** and **5** with respect to fragmentation ii. The molecular ion derived from phosphate **5** (m/e 466) is very stable and gives a base peak in the MS of **5**. It decomposes yielding all fragments expected for a triaryl phosphate; however, loss of the 4-nitrophenoxy radical (fragmentation ii) is not a favored one, since the 1-naphthyl 4-nitrophenyl phosphorylium ion (m/e 328) is formed only as a minor fragmentation product (relative abundance 4.6%). In the case of phosphate **4** the reverse is true; the molecular ion (m/e 467) is unstable (relative abundance ca. 7%), but the fragmentation ii is by far the most favored among all the available decomposition modes for this compound, and the corresponding phosphorylium ion (m/e 329) is formed as a base peak. Since in both cases fragmentation ii involves loss of the same species (PNPO·), it must be the relative stability of the ions formed, which determines the difference in the fragmentation behavior. Phosphorylium ions $(RO)_2P(O)^+$ are generally considered as unstable species,[19] so the low yield of fragmentation ii for **5** is not surprising. In system **4**, however, this fragmentation can be assisted by the heterocyclic nitrogen and the P–O bond cleavage (loss of PNPO·) results in the formation of the resonance-stabilized phosphorylium–ammonium ion **6a**.

(4)

6a
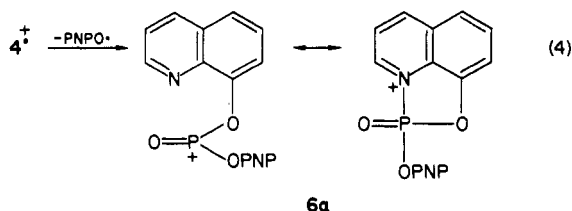
Alkaline Hydrolysis. Esters **4** and **5** were hydrolyzed in aqueous solutions of sodium hydroxide and the rates of reaction (5) were determined spectrophotometrically by monitoring the appearance of the 4-nitrophenoxide ion at 400 nm.

$$ArOP(O)(OPNP)_2 \xrightarrow{H_2O,\ OH^-}$$
$$(ArO)(PNPO)PO_2^- + PNPO^- \quad (5)$$
$$7$$
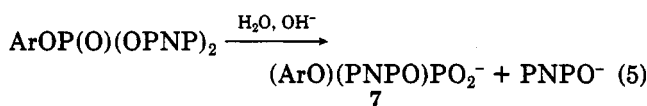
4, Ar = quinolin-8-yl

5, Ar = 1-naphthyl

Diesters **7** are sufficiently less reactive than the tertiary substrates for the reaction 5 to be conveniently followed without the possible interference of the hydrolysis of the second P–OPNP bond. Hydrolysis reactions were carried out in a large excess of NaOH in the absence of buffers, so the rate equation could be represented as

$$rate = k_{obsd}[S] \quad (6)$$

where the observed, pseudo-first-order rate constant

$$k_{obsd} = k_{spont} + k_{OH^-}[OH^-] \quad (7)$$

In the case of a simple ester (such as **5**), k_{spont} represents

(18) Gillis, R. G.; Occolowitz, J. L. In "Analytical Chemistry of Phosphorus Compounds"; Halman, M., Ed.; Wiley-Interscience: New York, 1972; Chapter 6.III.F.

(19) Haake, P.; Ossip, P. S. *J. Am. Chem. Soc.* **1971**, *93*, 6919.

Table III. Observed Rate Constants for the Hydrolysis in Aqueous NaOH at 25.0 °C ([S]$_o$ = 1.5 × 10^{-5} M)

[NaOH], M	$10^3 k_{obsd}$,[a] s^{-1}	
	4	5
0.0010	0.91	
0.0016	1.27	
0.0025	1.59	0.19
0.0037	2.38	0.29
0.0050	2.79	0.34
0.0075		0.53
0.010		0.68

[a] Average from 2–3 runs; ±3–6%.

rate constant for the hydrolysis by water alone, but for substrate **4** this, [OH$^-$] independent term, should also include any catalytic effects resulting from the presence of the quinolin-8-yl nitrogen atom. The obtained rates for the hydrolysis of phosphates **4** and **5** are summarized in Table III.

The plots of k_{obsd} vs. [OH$^-$] for **4** and **5**, are linear (r = 0.994 and 0.997, respectively), and the slopes and intercepts of these plots give the following values for the individual rate constants:

no.	$10^2 k_{OH^-}$ (s^{-1} M^{-1})	$10^2 k_{spont}$ (s^{-1})
4	47.8	0.046
5	6.5	0.0031

The phosphate ester derived from 8-hydroxyquinoline is more reactive than its 1-naphthyl analogue; however the increase in reactivity is not much different with respect to the "specific" rate constant, k_{OH^-} (k_{rel} = 7.3) and to the "spontaneous" rate constant k_{spont} (k_{rel} = 14.8). Although the intramolecular catalytic effect of the nitrogen is greater in phosphoric diesters than in triesters,[1] we believe that our results on hydrolysis provide no evidence for any significant specific effects of this type in ester **4**. The observed 7-fold increase in the k_{OH^-} value for **4** relative to **5** results from the inductive effect of the quinoline nitrogen atom, which increases the electron deficiency at the phosphorus atom and thus lowers the activation energy for the approach of a hydroxide ion. The values of k_{spont}, obtained from the intercepts of the plots have to be regarded as less accurate, so the value of k_{rel} = 15 has to be considered only as an approximate one. If the general, inductive effect of the quinoline nitrogen upon the rate of hydrolysis by neutral water were to be subtracted from the relative reactivity, the increase in the reactivity of **4** relative to **5** due to any "specific" catalytic effect by nitrogen should not exceed a factor of two. Such a rate enhancement (if any at all) contrasts sharply with the factor of 350 observed by Loran and Williams[2] for the analogous diesters. It seems, therefore, that the intermolecular approach of a strong, charged nucleophile (OH$^-$) to the phosphorus atom in a neutral ester is much more effective than the intramolecular strain involving attack of the tertiary nitrogen of the quinoline ring. In the aqueous medium, this nitrogen atom is certainly involved in hydrogen bonding to water, hence its nucleophilicity must be significantly decreased. Its ability to interact with the phosphoryl center via the five-membered cyclic system can be demonstrated in the solid state or in the gas phase, after the electron-impact induced activation of the molecule.

Experimental Section

Table IV. Crystal Data and Experimental and Refinement Parameters for the Structure Analyses

	5	4	4a
molecular formula	$C_{22}H_{15}N_2O_8P$	$C_{21}H_{14}N_3O_8P$	$C_{15}H_{11}N_2O_6P$
molecular weight, g mol^{-1}	466.35	467.34	346.24
space group	$P2_1/n$	$P\bar{1}$	$P\bar{1}$
a, Å	7.282 (4)	9.452 (3)	7.106 (7)
b, Å	12.683 (6)	8.751 (2)	9.559 (4)
c, Å	22.40 (1)	13.000 (3)	10.521 (4)
α, deg	90.00 (2)	100.59 (2)	84.32 (3)
β, deg	97.59 (2)	107.35 (2)	82.89 (10)
γ, deg	90.00 (2)	85.21 (2)	78.60 (7)
V, Å^3	2050.86	1008.43	693.12
Z	4	2	2
Dm, g cm^{-3}	1.45	1.52	1.65
Dc, g cm^{-3}	1.47	1.54	1.66
μ, cm^{-1}	(Cu K$_\alpha$)15.67	(Mo k$_\alpha$) 1.46	(Mo k$_\alpha$) 1.84
$F(000)$	960	480	356
crystal dimensions, mm^3	0.90 × 0.60 × 0.23	0.22 × 0.06 × 0.19	0.06 × 0.12 × 0.28
scan mode	$\omega - 2\theta$	$\omega - 2\theta$	$\omega - 2\theta$
scan width ($\Delta\omega$), deg	2.0	(0.64 + 0.35 tan θ)	(0.75 + 0.35 tan θ)
aperture width horiz	2°	(1.22 + 1.05 tan θ) mm	(1.29 + 1.05 tan θ) mm
vert.	1°	4 mm	4 mm
range scanned	6° ⩽ θ ⩽ 60°	1° ⩽ θ ⩽ 25°	1° ⩽ θ ⩽ 25°
stability of std refl	0.05%	1.46%	1.55%
no. of refl collected	3198	3713	2595
no. of obsd refl	2743 with $I_{(rel)} > 2\sigma I_{(rel)}$	1869 with $I_{(rel)} > 2\sigma I_{(rel)}$	1212 with $I_{(rel)} > 2\sigma I_{(rel)}$
no. of variables	301	301	192
$R = \sum \|\|F_o\| - \|F_c\|\|/\sum \|F_o\|$	5.23%	4.73%	5.58%
$R_w = \sum w^{1/2}\|\|F_o\| - \|F_c\|\|/\sum w^{1/2}\|F_o\|$	5.38%	4.49%	5.07%
weighting scheme	$(\sigma^2F)^{-1}$	$(\sigma^2F)^{-1}$	$(\sigma^2F)^{-1}$

operating at 70 eV and an ion source temperature of 200 °C. Electronic spectra were recorded on a Beckman UV-VIS 5260 spectrophotometer.

Melting points are uncorrected. All solvents and substrates used were AnalaR grade reagents and were purified in the usual manner.

1-Naphthyl Bis(*p*-nitrophenyl) Phosphate (5). To a stirred solution of 1-naphthyl phosphorodichloridate (prepared by refluxing a benzene solution of equimolar quantities of POCl$_3$, 1-naphthol, and pyridine; yield 82%; bp 150 °C (0.7 mm)) (0.02 mol) in dry ether (25 mL) the dry sodium *p*-nitrophenoxide (0.04 mol) was added at room temperature over a period of 30 min. The mixture was then refluxed for 2 h and cooled, and the precipitate filtered off and washed thoroughly with water. After drying, the crude product was recrystallized from ethanol–acetone: yield 60%; mp 118–120 °C. Anal. Calcd for $C_{22}H_{15}N_2O_8P$: C, 56.66; H, 3.20; N, 6.0. Found: C, 56.50; H, 3.35; N, 5.85. ^{1}H NMR (CDCl$_3$) was in full agreement with the expected structure.

Quinolin-8-yl Bis(*p*-nitrophenyl) Phosphate (4). To a stirred solution of bis(*p*-nitrophenyl) phosphorochloridate (prepared by nitration of diphenyl phosphochloridate;[20] yield 72%; mp 93–95 °C) (0.005 mol) in dry ether (10 mL) was slowly added the dry sodium salt of 8-hydroxyquinoline (0.005 mol). The mixture was then refluxed for 2 h and cooled, and the precipitate filtered off and washed with a small volume of water. After drying the crude product was recrystallized from benzene: yield 64%; mp 159–161 °C. Anal. Calcd for $C_{21}H_{14}N_3O_8P$: C, 53.97; H, 3.02; N, 8.99. Found: C, 53.90; H, 3.05; N, 8.80. ^{1}H NMR (CDCl$_3$) was in full agreement with the expected structure.

Quinolin-8-yl *p*-Nitrophenyl Phosphate (4a). This compound was prepared by condensation of 8-hydroxyquinoline with *p*-nitrophenyl phosphorodichloridate, followed by hydrolysis, as described by Loran and Williams.[2] Highly insoluble product (yield 79%) was recrystallized from a large volume of n-butyl alcohol and isolated as a monohydrate, mp 195–200 °C. Anal. Calcd for $C_{15}H_{14}N_2O_6P \cdot H_2O$: C, 49.44; H, 3.60; N, 7.69. Found: C, 49.35; H, 3.60; N, 7.80.

Crystals suitable for X-ray analysis were obtained by slow evaporation of an ethanol–chloroform solution of 5 and petroleum ether (80–100 °C)–chloroform solutions of 4 and 4a. Compound 4a was obtained in the anhydrous form. Crystal densities of all three compounds were measured by flotation.

Crystal Structure Analyses. The unit cell parameters and space group symmetries of compounds 5, 4, and 4a were initially determined photographically by using Weissenberg and precession single-crystal goniometers. Intensity data collections were then carried out on four-circle single-crystal diffractometers. Data for compound 5 were collected on a Philips PW 1100 by using Cu K$_\alpha$ radiation whereas a Nonius CAD4 with Mo K$_\alpha$ radiation was used for data collections of compounds 4 and 4a. Crystal data for all three structures were corrected for Lorentz polarization effects but not for absorption. The structures were solved by using direct methods (SHELX-76[21] and SHELXS-84[22] programs) and refined by successive least-squares and difference Fourier methods. Final refinements in structures 5 and 4 were carried out with all non-hydrogen atoms treated anisotropically and aromatic hydrogen atoms geometrically constrained. Structure 4a was refined with a mixture of anisotropic and isotropic thermal parameters assigned to the heavy atoms. Careful analysis of difference electron density maps showed N(19) to be protonated, thus producing a zwitterionic species with electronic delocalization on the two phosphoryl oxygens. In the final refinement H(19) was given a bond length constraint of N(19)–H(19) = 1.063 Å. This value was chosen as representing the typical hydrogen graph depicting N–H vs. N···O distances for a large number of structures.[23] Refinement parameters are given in Table IV.

Rate Measurements. All kinetic measurements were done spectrophotometrically by recording the increase in absorbance at 400 nm due to the appearance of *p*-nitrophenoxide ion. In a typical run, 3 mL of the aqueous NaOH solution was pipetted into a 1-cm quartz cell and allowed to thermally equilibrate by keeping it in the sample compartment which was thermostatted at 25.0 °C. The reaction was initiated by injecting 25 µL of the dioxane solution of a substrate into the reaction solution. The substrate concentration was ca. 1.5 × 10^{-5} M and sodium hydroxide was used in 67–667-fold molar excess. The observed pseudo-first-order rate constants (k_{obsd}) were obtained by linear regression as the slope of the plots of ln ($A_\infty - A_t$) against time. A_t is absorbance at time t and A_∞ is absorbance at infinite time, measured after 10 half-lives. In this way the hydrolysis of the

(20) Murayama, A.; Jastorff, B.; Cramer, F.; Hettler, H. *J. Org. Chem.* **1971**, *36*, 3029.

(21) Sheldrick, G. M. The SHELX program in "Computing in Crystallography"; Schenk, H.; Olthof-Hazenkamp, R., van Koningsveld, H., Bassi, G. C., Eds.; Delft University Press: Delft, 1978.

(22) Sheldrick, G. M. SHELXS-84 Direct Methods Program. Preliminary version. Private Communication, 1983.

(23) "The Hydrogen Bond"; Schuster, P., Zundel, G., Sandorfy, C., Eds.; North-Holland Publishing Co.: Amsterdam, 1976; Vol. 11, p 412.

first P–ONP linkage was monitored. In all cases, linear plots were obtained, to at least 80% reaction with typical correlation coefficients 0.997–0.999. Rate constants were reproducible to 3–6% of the average value.

Reductive Dimerizations of Perchlorofluorene. Synthesis of an Overcrowded, Twisted Ethylene

M. Ballester,* J. Castañer, J. Riera, G. de la Fuente, and M. Camps

Instituto de Química Orgánica Aplicada (C.S.I.C.), C. Jorge Girona Salgado 18-26, 08034 Barcelona, Spain

Perchloro-9,9'-bifluorenylidene (**2**), a highly twisted ethylene, has been synthesized from perchlorofluorene (**3**) with Cu at 280 °C or from 9H-heptadecachloro-9,9'-bifluorenyl (**1**) by dehydrochlorination with NaOH. **1** has been obtained from **3** with SnCl₂. In spite of the high angle of twisting (67°), **2** is a diamagnetic chlorocarbon (magnetic susceptibility and ESR), i.e., a singlet. Hydrogenation of **2** gives 9H,9'H-hexadecachloro-9,9'-bifluorenyl (**8**). From **2** chlorocarbons perchlorobenzo[e]indeno[1,2,3-*hi*]acephenanthrylene (**5**), perchloro-14b,14c-dihydrobenzo[e]indeno[1,2,3-*hi*]acephenanthrylene (**4**), and perchloro-2,2',3,3'-tetrahydro-1H,1'H-9,9'-bifluorenyl (**10**) have been obtained. The preceding compounds have given rise, either directly or indirectly, to perchlorofluorenone (**12**), perchloro-3,3'-dioxo-9,9'-bifluorenyl (**13**), perchloro-9-(3-oxo-9-fluorenyl)-1-fluorenone (**14**), tetradecachloro-3,3'-dihydroxy-9,9'-bifluorenylidene (**15**), tetradecachloro-1,3'-dihydroxy-9,9'-bifluorenylidene (**16**), 3,3'-diacetoxytetradecachloro-9,9'-bifluorenylidene (**17**), 1,3'-diacetoxytetradecachloro-9,9'-bifluorenylidene (**18**), and tetradecachloro-3,3'-dimethoxy-9,9'-bifluorenylidene (**19**). Chemical and ESR evidence for the formation of perchlorofluorenyl (PF) and 9H-octachlorofluorenyl (**21**) radicals is given, and the frontal strain of the relevant dimers is discussed. In the mechanistic interpretation of some reactions here reported, the role of steric distortion and shielding, due to chlorine overcrowding, is considered.

It has been reported that (trichloromethyl)benzenes such as *o*-H-heptachlorotoluene,[1] *p*-H-heptachlorotoluene,[2] and perchlorotoluene,[1,3,4] are reduced by iodide ion, by stannous chloride, or by ferrous chloride to give dimers and/or dimeric products therefrom. Those reactions take place through α,α-dichlorobenzyl radicals which yield α,α,α',α'-tetrachlorobibenzyls and/or α,α'-dichlorostilbenes. When the trichloromethyl group is flanked by *two ortho* chlorines, the isolated product is invariably a mixture of *cis*- and *trans*-α,α'-dichlorostilbenes, and this is due to frontal steric strain in the intermediate bibenzyl which favors vicinal chlorine elimination. If there is only *one ortho* chlorine, a mixture of the bibenzyl and the stilbenes is obtained.[1] In the case of perchlorotoluene (stannous chloride), the intermediate perchlorobenzyl has been detected by ESR spectrometry and found to be, at room temperature, in equilibrium with its dimer, the perchlorobibenzyl.[4]

Such a type of reduction takes place with the perchlorodiphenylmethane as well.[5,6] Nevertheless, the isolated product is neither the perchlorotetraphenylethane nor the perchlorotetraphenylethylene, as it might be expected, but the perchlorodiphenylmethyl radical (PDM), a historical precursor of the "inert carbon free radicals".[5,6] This result is due to a prohibitive frontal strain in the hypothetical dimer of PDM. Similarly, the reduction of perchloro-9-phenylfluorene by ferrous chloride *does not* give dimeric products but inert perchloro-9-phenylfluorenyl radical (PPF),[7] and this is attributed to steric shielding of the 9-carbon by its four proximal chlorine atoms.

In spite of this hindrance to dimerization, and in connection with the problem of ethylene-bond twisting, it was regarded of significance to attempt the synthesis of related tetrasubstituted ethylenes provided with strong steric repulsions among their substituents.

It was reported long ago that steric interactions between the carbon pairs 1/1' and 8/8' in hydrocarbon 9,9'-bifluorenylidene are very significant,[8] the central ethylene (9,9') bond being twisted about 42°.[9] Such a twisting confers a red color to that hydrocarbon, as well as thermochromy. Therefore, it was decided to attempt the

(1) Ballester, M.; Molinet, C.; Rosa, J. *Tetrahedron* **1959**, *6*, 109.
(2) Ballester, M.; Rosa, J. *An. R. Soc. Esp. Fís. Quim.*, *Ser. B* **1960**, *56*, 203.
(3) Ballester, M. *Bull. Soc. Chim. Fr.* **1966**, 7.
(4) Olivella, S.; Ballester, M.; Castañer, J. *Tetrahedron Lett.* **1974**, 587.
(5) Ballester, M.; Riera, J. *J. Am. Chem. Soc.* **1964**, *86*, 4505.
(6) Ballester, M.; Riera, J.; Castañer, J.; Badía, C.; Monsó, J. M. *J. Am. Chem. Soc.* **1971**, *93*, 2215.

(7) Ballester, M.; Castañer, J.; Riera, J.; Pujadas, J.; Armet, O. *J. Org. Chem.* **1984**, *49*, 770.
(8) Bergmann, E. D. *J. Chem. Soc.* **1935**, 987. Bergmann, E. D.; Berthier, G.; Pullman, A.; Pullman, M. B. *Bull. Soc. Chim. Fr.* **1950**, *17*, 1079. Rabinovitz, M.; Agranat, I.; Bergmann, E. D. *Tetrahedron Lett.* **1965**, 1265.
(9) Bailey, N. A.; Hull, S. E. *Acta Crystallogr.*, *Sect. B* **1978**, *B34*, 3289.